Non-Axisymmetric Radiation from Surface-Wave Oscillator Driven by Weakly Relativistic Electron Beam*)

Yuta ANNAKA, Kazuo OGURA, Kosuke OZAWA, Makoto NAKASONE and Yuki SATO

Graduate School of Science and Technology, Niigata University, Niigata 950-2181, Japan

(Received 6 September 2018 / Accepted 24 November 2018)

In this paper, non-axisymmetric radiation from a W-band surface wave oscillator (SWO) is observed. The SWO is based on a cylindrical corrugated waveguide with a periodic structure on its inner wall. This SWO is driven by electron beams with energy of less than 100 keV and a current on the order of 100 A. The waveguide has transverse magnetic (TM) and transverse electric (TE) modes as its axisymmetric normal modes. Non-axisymmetric modes also appear as a hybrid of TM and TE modes and form surface waves near the periodic structure. The frequencies of the non-axisymmetric modes increase as the azimuthal mode number m increases. By injecting an annular electron beam into the SWO, many non-axisymmetric modes with m up to 30 are excited and intense radiation is generated at frequenies up to 140 GHz.

Keywords: terahertz wave source, surface wave oscillator, corrugated waveguide, non-axisymmetric mode

DOI: 10.1585/pfr.14.2406015

1. Introduction

Terahertz-wave sources are in demand for applications such as non-destructive inspection, wireless communication, radar systems, and plasma control. Slow-wave devices are among the most promising high-power sources of terahertz waves [1]. These devices are based on a periodic structure in which the kinetic energy of an electron beam is converted into electromagnetic (EM) wave energy. The surface-wave oscillator (SWO) is a slow-wave device utilizing a cylindrical corrugated waveguide [2–5]. This corrugated waveguide has two axisymmetric normal modes: transverse magnetic (TM) and transverse electric (TE). Non-axisymmetric normal modes are a hybrid of TM and TE modes and have the phase factor $\exp(im\theta)$, where m is the azimuthal mode number and θ is the azimuthal angle. Many non-axisymmetric modes with various m values arise in a cylindrical corrugated waveguide. A corrugated waveguide has a periodic structure on its inner wall. This structure reduces a phase velocity of EM wave slower than that of light. Both axisymmetric and non-axisymmetric modes may become a slow wave. The intensity distribution of the slow wave is concentrated on the surface of the structure when the corrugated waveguide is oversized: the inner radius of the waveguide is several times larger than the wavelength of an EM wave in free space. Such wave is called a surface wave. By injecting an electron beam into the waveguide, axisymmetric and non-axisymmetric surface-wave modes can be excited to generate intense radiation [6]. When many non-axisymmetric modes exist close to each other, we have a serious problem, so called mode competition problem, which degrade device performance [7, 8]. In order to understand the multimode nature of SWO, the characteristics of emanating from many non-axisymmetric modes should be investigated.

In this study, we examine the excitation of non-axisymmetric surface-wave modes in a W-band SWO. The frequency of a non-axisymmetric mode increases with the increase in the mode number m. The upper cutoff frequency of the non-axisymmetric mode with $m = 30$ is 140 GHz, whereas that of the axisymmetric TM_{01} mode is 100 GHz. Non-axisymmetric radiation with higher frequencies are observed using the detecting systems with high-pass filters at cutoff frequencies of 74, 116, and 137 GHz. An electron beam is generated by applying a voltage pulse lower than 100 kV to a cold cathode, yielding a current on the order of 100 A.

2. Experimental Setup

In our experimental setup, a disk-type cold cathode and a corrugated waveguide are placed in a vacuum chamber. By applying voltage to the cathode, an electron beam is generated and is injected axially into the corrugated waveguide. A schematic of the corrugated waveguide with an axially propagating electron beam is shown in Fig. 1. The corrugated waveguide is made of aluminum and has a rectangular periodic structure on its inner wall. The size parameters of the structure are an average radius $R_0 = 15.1$ mm, a corrugation amplitude $h = 0.3$ mm, a periodic length $z_0 = 0.5$ mm, and a groove width $d = 0.3$ mm. The beam limiter, with an inner diameter of 29.7 mm, is connected in front of the corrugated waveguide and functions as an anode. The cold cathode is located 10 mm away

author's e-mail: annaka@eng.niigata-u.ac.jp

*) This article is based on the presentation at the 12th International Conference on Open Magnetic Systems for Plasma Confinement (OS2018).

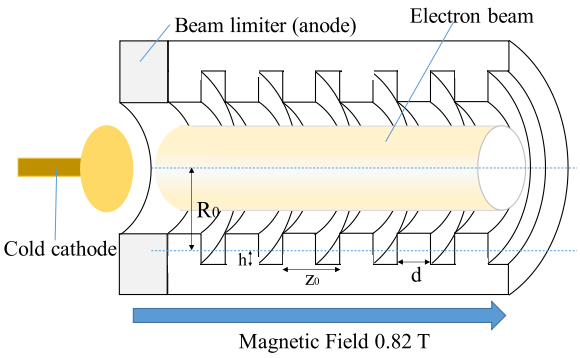

Fig. 1 Schematic of corrugated waveguide with beam diode and axially propagating annular electron beam. Beam diode is composed of cold cathode and beam limiter.

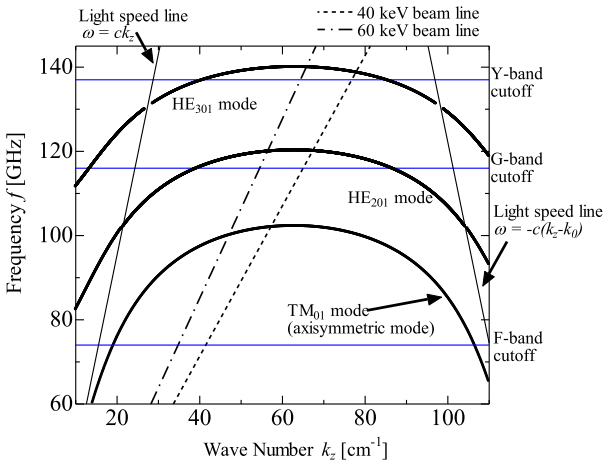

Fig. 2 Dispersion curves of axisymmetric TM_{01} mode and non-axisymmetric HE_{201} and HE_{301} modes.

from the anode. This cathode is made of oxygen-free copper and its diameter is 29.0 mm. In order to generate an annular electron beam, a dielectric fiber is attached to the edge of the cathode surface [9, 10]. The pulse-forming line is connected to the cathode and the voltage pulse up to 100 kV is applied to the cathode. A 0.82 T uniform magnetic field is generated by 10 solenoid coils. A beam current is measured by a Rogowski coil.

Intense radiation is generated while the electron beam propagates within the corrugated waveguide. The radiation passes to the outside of the vacuum chamber through an output window and is observed by F-band, G-band and Y-band detecting systems. F-band, G-band and Y-band are EIA standard. The detecting system is composed of a horn antenna, a rectangular waveguide, a directional coupler, and a crystal diode detector. The rectangular waveguides have cutoff frequencies and serve as high-pass filters. The cutoff frequencies are 74 GHz for the F-band, 116 GHz for the G-band, and 137 GHz for the Y-band. The directional coupler is used as a 20-dB attenuator in the F-band system although no directional coupler is used in the G-band and Y-band systems. The diode detectors are ELVA-1 ZBD-08 for the F-band, Pacific Millimeter Product GD for the G-band and ELVA-1 ZBD-06 for the Y-band. The output voltages of the ELVA-1 ZBD-08 and ZBD-06 detectors are calibrated to the absolute values of power using a Gunn oscillator at 100 GHz. The output voltage of the G-band detector is calibrated to the absolute value of power by a G-band BWO [11]. The detecting systems are located 600 mm away from the window.

3. Non-Axisymmetric Mode

Non-axisymmetric modes are a hybrid of TM and TE modes and are commonly designated by the letters EH and HE. The definitions of EH and HE are arbitrary. In this study, we use the definition common in plasma physics research: The TM mode is dominant in The EH mode and the TE mode is dominant in the HE mode [12]. Using numerical code developed in Ref. [13], the dispersion curves of the waveguide modes are calculated from the size parameters and are shown in Fig. 2. In this figure, the vertical axis represents the frequency f and the horizontal axis represents the wavenumber k_z. The dispersion curves indicate the axisymmetric TM_{01} mode and the non-axisymmetric HE_{m1} modes with $m = 20$ and 30. The upper cutoff frequencies of the modes appear at $k_z = 62.83\,\mathrm{cm}^{-1}$ and are 100 GHz for $m = 0$, 120 GHz for $m = 20$, and 140 GHz for $m = 30$. The thin solid lines plot the light lines for $\omega = ck_z$ and $\omega = -c(k_z - 2\pi/z_0)$, where $\omega = 2\pi f$ is the angular frequency and c is the velocity of light. The phase velocities of the non-axisymmetric modes ω/k_z are slower than c, so these HE modes are slow waves. As mentioned in Sec. 1, slow waves are surface waves on the vicinity of the periodic structure. The dashed and dash-dotted lines indicate the 40 and 60 keV beam lines $\omega = vk_z$, respectively, where v is the beam velocity. The electron beam interacts with a non-axisymmetric mode at the intersection of the beam line and dispersion curve, leading to intense radiation. The electron beam in an oversized corrugated waveguide interacts with the TM modes, but not with the TE modes. The TM mode becomes dominant in the HE_{m1} mode in the slow-wave region in which the phase velocity is slower than c and an electron beam interacts with HE_{m1} modes, whereas the TE mode is dominant in HE mode around $k_z = 0$ [14]. No EH modes become surface waves at frequencies below 150 GHz, so these may not contribute to radiation. The blue solid lines indicate the cutoff frequencies of the detecting systems that were discussed in Sec. 2. The upper cutoff the frequencies of HE_{m1} modes are plotted as a function of the mode number m in Fig. 3. The frequencies of HE_{m1} modes increase as the mode number m increases. Radiation may be observed when the frequency is sufficiently larger than the cutoff frequencies of the detecting systems. The G- and Y-band detecting systems are expected to observe radiations with mode number m larger than 20 and 30, respectively.

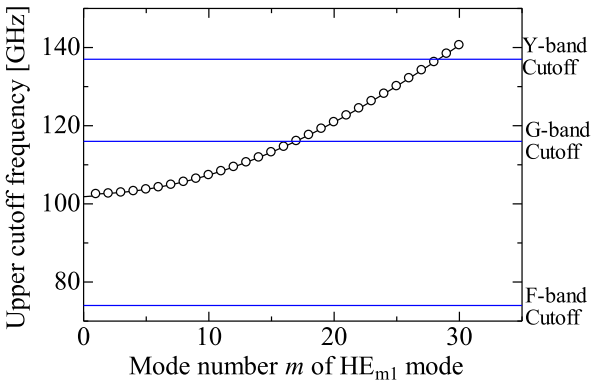

Fig. 3 Dependence of upper cutoff frequency of HE_{m1} mode on mode number m.

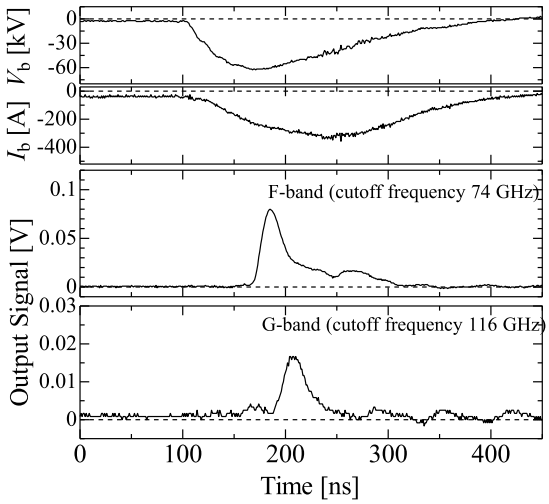

Fig. 4 Temporal evolution of cathode voltage, beam current, and F- and G-band signals.

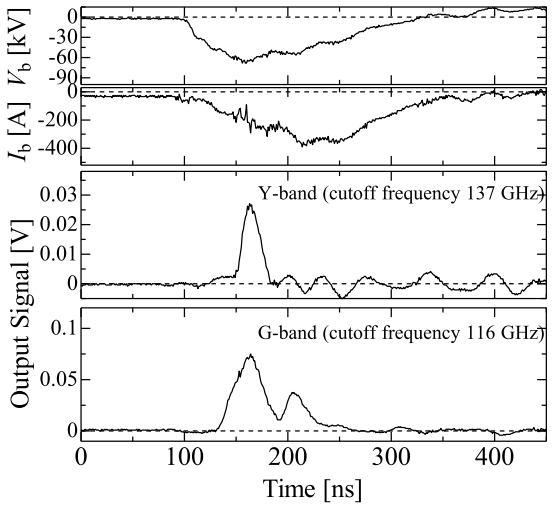

Fig. 5 Temporal evolution of cathode voltage, beam current, Y- and G-band signals.

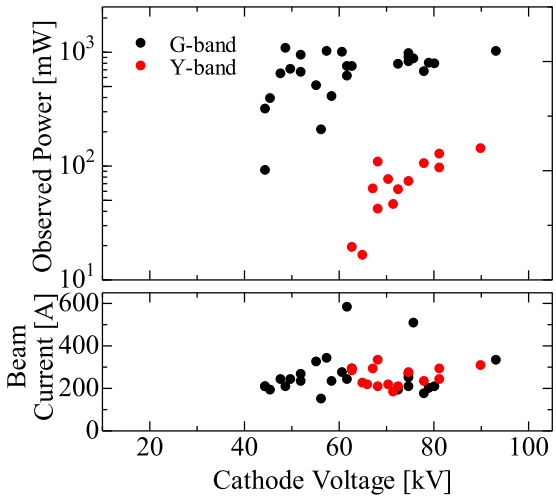

Fig. 6 Dependence of G- and Y-band observed power and beam current on cathode voltage.

4. Experimental Result

With an electron beam injected into the corrugated waveguide, the time evolution of the cathode voltage, the beam current, and the output signals of the F-band and G-band detectors are obtained as shown in Fig. 4. The F-band signal is decreased by a 20-dB attenuator. The peak of F-band signal is observed at 185 ns where the cathode voltage is 79 kV and beam current 257 A. The observed F-band peak power is 760 mW. The peak of the G-band signal is observed at 210 ns where the cathode voltage is 68 kV and the current is 290 A. The observed peak of the G-band power is 166 mW. Signals from the G- and Y-band detecting systems are shown in Fig. 5. Their maximum values appear at the same time at 163 ns, when the cathode voltage and current are 65 kV and 224 A, respectively. The observed power at 163 ns is 749 mW for the G-band and 16 mW for the Y-band. Considering the cutoff frequencies of the G- and Y-band systems, the frequencies are over 116 GHz for G-band radiation and 137 GHz for Y-band radiation. The second peak in the G-band signal appears at 204 ns, at which point the cathode voltage and current are 55 kV and 299 A, respectively. The G-band power at 204 ns is 374 mW. No meaningful Y-band signal is observed around 204 ns. In accordance with the cutoff frequencies, the frequency of the G-band radiation lies in the range from 116 to 137 GHz. By varying the cathode voltage, the peak values of the G- and Y-band signals and the beam current at the corresponding time are plotted as the function of the cathode voltage in Fig. 6. In order to collect the data, over 50 shots are observed. The beam currents are distributed between 100 and 600 A. G-band radiation is detected in the voltage region above 40 kV. The maximum observed power is on the order of 1 W. On the other hand, Y-band radiation is observed in the voltage range above 60 kV. The maximum observed power is on the order of 0.1 W.

Intense radiation is observed by G- and Y-band detecting systems with cutoff frequencies of 116 and 137 GHz, respectively. G-band radiation is observed with cathode voltages above 40 kV, and Y-band radiation is observed with cathode voltages above 60 kV. The G-band power level is 10 times higher than the Y-band. As the data in Figs. 2 and 3 show, the G-band signals in Figs. 4, 5, and 6 correspond to the excitation of HE_{m1} modes with m above 20. Likewise, the Y-band signals in Figs. 5 and 6 may result from the excitation of HE_{m1} modes with mode numbers m above 30.

These experimental data show that many HE_{m1} modes are excited, with m up to at least 30. By comparing the power levels of the G- and Y-band signals, the intensity of non-axisymmetric radiation appears to decrease as the mode number m increases from 20 to 30. Hence, the radiation with the lowest azimuthal mode number may be dominant in these signals. In other words, radiation with $m = 20$ and 30 seems to be dominant in the G- and Y-band signals, respectively. As Fig. 6 shows, G- and Y-band radiation is detected with cathode voltages above 40 and 60 kV, respectively. This result suggests that a threshold cathode voltage for non-axisymmetric radiation exists and that this threshold value increases as the mode number m increases. In Fig. 5, the Y-band signal disappears around 204 ns, although a G-band signal is observed. At this moment, the cathode voltage is 55 kV and the signal is over the threshold value for $m = 20$ but below the threshold for $m = 30$.

5. Discussion and Conclusion

F-band signals are observed from around 10 kV and correspond to the W-band oversized SWO oscillation presented in Ref. [2]. This oversized SWO has been shown to be a multimode system through radiation pattern measurements. We observed the excitation of many HE_{m1} modes up to $m = 30$ on the basis of the difference among their frequencies. The multimode nature of our oversized SWO leads to the existence of many non-axisymmetric modes. In Fig. 4, the F-band power level is about 4.6 times greater than the G-band power level. This difference results from the fact that the F-band signal may include radiation in the TM_{01} and HE_{m1} modes with mode numbers m greater than 1. Although the F-band detector is sensitive enough to detect radiation up to $m = 30$, the main contribution to non-axisymmetric modes comes from radiation with m much less than 20, which exist very closely to the TM_{01} mode.

In conclusion, our experiment returned novel data about non-axisymmetric radiation from a W-band SWO. Non-axisymmetric HE_{m1} modes with a range of azimuthal mode numbers m form surface waves on the surface of the SWO's periodic structure. When an annular electron beam is injected into the SWO, many HE_{m1} modes are excited. Intense radiation due to the excitation of non-axisymmetric HE_{m1} modes with azimuthal mode numbers up to $m = 30$ are observed. We conclude that non-axisymmetric radiation is generated when the cathode voltage is over a certain threshold. This threshold value increases as the mode number m increases. The results presented above contribute to our understanding of the multimode nature of SWO and to solving the mode competition problem. This solution will have an important effect on the development of terahertz-wave sources.

[1] J.H. Booske, Phys. Plasmas **15**, 055502 (2008).
[2] Min Thu San *et al*., Plasma Fusion Res. **11**, 2406085 (2016).
[3] N.S. Ginzburg *et al*., Phys. Rev. Lett. **117**, 204801 (2016).
[4] Min Thu San *et al*., IEEE Trans. Plasma Sci. **45**, 30 (2017).
[5] J. Wang *et al*., Sci. Rep. **8**, 6978 (2018).
[6] K. Ogura *et al*., J. Plasma Fusion Res. SERIES **6**, 703 (2004).
[7] K. Mizuno *et al*., IEEE Trans. Electron Devices **20**, 749 (1973).
[8] T.M. Antonsen, Jr. and B. Levush, Phys. Rev. Lett. **62**, 1488 (1989).
[9] H. Oe *et al*., J. Plasma Fusion Res. SERIES **8**, 1477 (2009).
[10] K. Yambe *et al*., IEEE Trans. Plasma Sci. **41**, 2781 (2013).
[11] S. Magori *et al*., Plasma Fusion Res. **9**, 3406032 (2014).
[12] O. Watanabe *et al*., Phys. Rev. E **63**, 056503 (2001).
[13] Y. Takashima *et al*., J. Plasma Fusion Res. SERIES **8**, 1512 (2009).
[14] H. Yamazaki *et al*., J. Plasma Phys. **72**, 915 (2006).